AIAA JOURNAL
Vol. 30, No. 3, March 1992

Effect of Airfoil (Trailing-Edge) Thickness on the Numerical Solution of Panel Methods Based on the Dirichlet Boundary Condition

Steven Yon,* Joseph Katz,† and Allen Plotkin†
San Diego State University, San Diego, California 92182

Computational methods based on the solution of the potential flow model are widely used for the analysis of low-speed, inviscid, attached-flow problems. Most of such recent methods are based on the implementation of the internal Dirichlet boundary condition instead of the zero normal flow on a solid-surface (frequently called the Neumann) boundary condition. These methods, however, were developed for thick wings and bodies and become singular as the thickness approaches zero. In this article the practical limit of airfoil thickness ratio for which acceptable engineering results are obtainable with the Dirichlet boundary-condition-based numerical methods is investigated. This is done by studying the effect of thickness on the calculated pressure distribution near the trailing edge and by comparing the aerodynamic coefficients with available exact solutions. The first objective of this study, owing to the wide use of such computational methods, is to demonstrate the numerical symptoms that occur when the body or wing thickness approaches zero and to increase the awareness of potential users of these methods. Additionally, an effort is made to obtain the practical limits of the trailing-edge thickness where such problems will appear in the flow solution, and to propose some possible cures for very thin airfoils or those with cusped trailing edges.

Introduction

THE applicability of inviscid flow models for a large variety of high-Reynolds-number fluid dynamic problems is widely recognized by the engineering community. In recent years this approach led to the development of numerous numerical solutions based on these principles which are called *panel methods*. These numerical solutions differ from each other primarily in the type of boundary condition utilized, in the order of approximation for the singularity strength distribution, and in how the shape of the solid surface is defined (for a description of several such panel elements, see, for example, Ref. 1, Chap. 11). Recent trends, however, indicate that the use of the internal Dirichlet boundary condition[2,3] is gaining popularity as a result of its simpler formulation and smaller computational effort (see Fig. 11.36 in Ref. 1). These methods have proved to be successful when treating thick wings and bodies, but when the thickness approaches zero (e.g., for a wing near its trailing edge), then the solution may become singular (as pointed out by Morino and Kuo[2]).

Because of the wide use of such codes[4–6] by the engineering/research community, the primary objectives of this study are:

1) Investigate the practical limits of airfoil thickness when using panel codes based on the Dirichlet boundary condition so that potential users of such codes will be aware of such problems.

2) Propose some possible cures to the problem for thin airfoils having very thin or cusped trailing edges.

Basic Formulation

The potential flow model, which provides the foundation for panel methods, is based on the assumption that for a high-Reynolds-number flow the fluid outside a very thin boundary layer (on the body's surface) can be assumed to be inviscid, incompressible, and irrotational (potential flow). To briefly present this model, we consider a body with known boundaries S_B submerged in such a potential flow, as shown in Fig. 1. The flow of interest is in the outer region where the incompressible continuity equation in terms of the total velocity potential Φ^* is

$$\nabla^2\Phi^* = 0 \tag{1}$$

For simplicity we shall consider the two-dimensional‡ case only, and following Green's second identity (Ref. 1, Sec. 3.2) the general solution to Eq. (1) can be constructed by a sum of source σ and doublet μ distributions placed on the surface of the boundary S (which includes S_B and possibly a wake surface S_W):

$$\Phi^*(x, z) = \frac{-1}{2\pi}\int_S [\sigma(\ln r) - \mu \boldsymbol{n}\cdot\nabla(\ln r)]\mathrm{d}S + \Phi_\infty \tag{2}$$

Here r is the distance between the source (or doublet) element and a field point, the vector $\boldsymbol{n}$ is normal to S and points in the direction of the potential jump μ and is positive when it

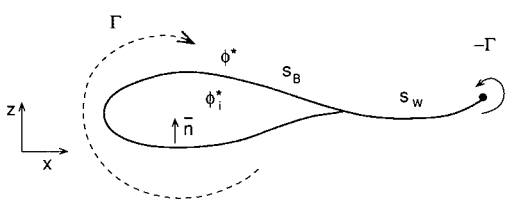

Fig. 1 Nomenclature used to define the mathematical problem.

Received March 2, 1991; revision received June 17, 1991; accepted for publication June 21, 1991. This paper is declared a work of the U.S. Government and is not subject to copyright protection in the United States.

*Graduate Student, Department of Aerospace Engineering and Engineering Mechanics. Student Member AIAA.

†Professor, Department of Aerospace Engineering and Engineering Mechanics. Associate Fellow AIAA.

‡It will be shown later that numerical instabilities initiate near the trailing edge where (even for three dimensional wings) the two-dimensional Kutta condition is usually specified. Therefore, it is assumed that for the purpose of this study a two dimensional treatment of the problem is sufficient.

points inside the body (Fig. 1), and Φ_∞ is the freestream potential:

$$\Phi_\infty = U_\infty x + W_\infty z \tag{3}$$

The "direct" boundary condition on the surface requires that the velocity component normal to the solid surface S_B be zero:

$$\nabla\Phi^* \cdot \boldsymbol{n} = \nabla(\Phi + \Phi_\infty) \cdot \boldsymbol{n} = 0 \tag{4}$$

and Φ is the perturbation potential [the integral term in Eq. (2)]. Also, the terminology "total potential" becomes evident now since $\Phi^* = \Phi + \Phi_\infty$.

A second boundary condition (at the distant, outer boundaries of the flow) requires that the flow disturbance, due to the body's motion through the fluid, should diminish far from the body:

$$\lim_{r\to\infty} \nabla\Phi = 0 \tag{5}$$

This condition is automatically met by all the singular solutions presented in Eq. (2).

Note that if for an enclosed boundary (e.g., S_B) $\partial\Phi^*/\partial n = 0$, as required by the boundary condition in Eq. (4), then the potential inside the body will not change (e.g., see Ref. 7, theorem 4, p. 216):

$$\Phi_i^* = \text{const} \tag{6}$$

This equation is the Dirichlet boundary condition for Eq. (2) and is an alternate form of Eq. (4).

To solve this mathematical problem, a combination of source/doublet distributions is placed along S_B with a wake model for the discontinuity of the velocity potential on S_W (consisting of doublets only) and the Kutta condition will be specified at the trailing edge. This condition requires that the pressure difference at the trailing edge (TE) of an airfoil be zero and traditionally this was formulated by requiring that the circulation density at the trailing edge be equal to zero ($\gamma_{TE} = 0$) which in terms of doublets (see Ref. 1, Sec. 9.3) becomes

$$\mu_U - \mu_L = \mu_W = \text{const} \tag{7a}$$

An alternate formulation is possible by requiring that the velocity will be equal for the upper (subscript U) and lower (subscript L) trailing-edge surfaces. In terms of the surface doublet distribution near the trailing edge this can be expressed as

$$\frac{\partial\mu_U}{\partial S} = \frac{\partial\mu_L}{\partial S} \tag{7b}$$

where S is the coordinate along the upper or lower surfaces.

For the purpose of numerical solution the basic panel element is represented by a constant strength singularity distribution placed along a straight line segment (this approach is widely used in many panel codes), and the body is now divided into N such surface panels, and the wake to N_W panels (see Fig. 2 where only one wake panel is used, but in cases such as the multielement airfoil at least one wake panel for each airfoil's trailing edge is required). The boundary condition will be specified at each of the body's surface elements at a "collocation point" (which for the Dirichlet boundary condition is specified inside the body). After rewriting the Dirichlet boundary condition for each of the N collocation points [with the use of Eq. (2) for the potential of each panel] the following discretized formulation is obtained:

$$\sum_{k=1}^{N} C_k\mu_k + \sum_{l=1}^{NW} C_l\mu_l + \sum_{k=1}^{N} B_k\sigma_k = 0 \tag{8}$$

for each collocation point k, where the coefficients B_k and C_k are a result of the integration on each panel and depend on the panel geometry. For example, for a constant strength μ element the influence of panel k (lying between points 1 and 2) at an arbitrary field point (x, z) is

$$\frac{1}{2\pi}\int_{1,2} \frac{\partial}{\partial n}(\ell n r)\mathrm{d}S|_k \equiv C_k \tag{9}$$

and for a constant strength σ element

$$\frac{-1}{2\pi}\int_{1,2} (\ell n r)\mathrm{d}S|_k \equiv B_k \tag{10}$$

These equations depend on the field point and the panel coordinates only and this can be demonstrated for the case of the doublet by performing the integration in Eq. (9):

$$C_k = \frac{-1}{2\pi}\left[\tan^{-1}\frac{z - z_2}{x - x_2} - \tan^{-1}\frac{z - z_1}{x - x_1}\right] \equiv \frac{-1}{2\pi}(\theta_2 - \theta_1) \tag{11}$$

where θ_1, θ_2 are the angles between the panel edges and the field point. When the field point of interest is on the element then this equation becomes

$$C_k = \mp\tfrac{1}{2} \tag{12}$$

where the plus sign is used when the panel is approached from below the element (from inside the body).

Equation (8) is the numerical equivalent of the boundary condition. If the strength of the sources is selected (e.g., $\sigma_k = -\boldsymbol{n}_k \cdot \boldsymbol{V}_\infty$ for the case of $\Phi_i^* = \Phi_\infty$ and $\boldsymbol{V}_\infty = (U_\infty, W_\infty)$, see Ref. 1, p. 241) then the coefficients B_k can be computed and the strengths σ_k are known and the last term in Eq. (8) can be moved to the right-hand side of the equation. Thus Eq. (8), when specified for the N collocation points, results in a set of N linear algebraic equations with $N + 1$ unknowns: $\mu_1 \ldots \mu_N$, μ_W (and for the single airfoil only one wake panel is used here). An additional equation for the wake doublet strength ($\mu_W = \mu_N - \mu_1$) is constructed by using the Kutta condition [Eq. (7a)] and the resulting $N + 1$ equations can be solved by standard algebraic methods.

The solution of the matrix equation provides the doublet values of each of the N panels and the pressure coefficient for each panel can be calculated by using Eq. (13):

$$C_p = 1 - \frac{V_t^2}{V_\infty^2} \tag{13}$$

where V_t is the tangential velocity component at the panel outer surface due to the freestream and the perturbation velocity potentials [$V_t = V_{\infty_t} + (\partial\mu/\partial S)$]. The contribution of each panel to the force component in the x and z directions is then

$$\Delta C_{xk} = -C_{pk}\Delta S_k \sin\theta_k \tag{14a}$$

$$\Delta C_{zk} = -C_{pk}\Delta S_k \cos\theta_k \tag{14b}$$

where the panel length ΔS_k and inclination θ_k are shown in Fig. 2. The total lift and moment are obtained by summing the contribution of each element and relating them to the freestream direction. Note that the lift can be calculated by using the Kutta-Joukowski theorem

$$L = \rho V_\infty \Gamma = \rho V_\infty \Gamma_W \tag{15}$$

and since the wake is modeled by a constant strength doublet its strength is equal to the strength of the starting vortex (see Fig. 2)

$$\Gamma_W = \mu_W \tag{16}$$

which according to Kelvin's theorem ($d\Gamma/dt = 0$) is equal to the airfoil's circulation.

Results and Discussion

The practical solution of the flowfield over airfoils includes considerations involving the modeling of the viscous boundary layer, its displacement thickness, or models for finite thickness or even diverging trailing edges. The current discussion, however, is limited to the phase where these considerations have resulted in a surface geometry that will be used for the potential flow solver. The quality of the numerical solution for this surface geometry is then investigated by comparing the computed results with available exact solutions.

To demonstrate the effect of thickness on the numerical solution, the van de Vooren airfoil shape is selected for which the exact (analytic) pressure distribution and lift are presented in Ref. 1, Chap. 6. This airfoil shape (shown in Fig. 3) is similar to the Joukowski airfoil (which has a cusped trailing edge), but its trailing edge angle is finite and, therefore, is more suitable for numerical calculations. The constant-strength singularity panel element described in this article is similar to the elements used in some of the widely used panel codes (e.g., Ref. 4–6) and therefore the following results can provide some guidelines for the users of such panel methods.

The pressure distribution on the upper and lower surfaces of the van de Vooren airfoil for various thickness ratios is presented in Fig. 4 and for these calculations the more common form of the Kutta condition was used [Eq. (7a)]. The

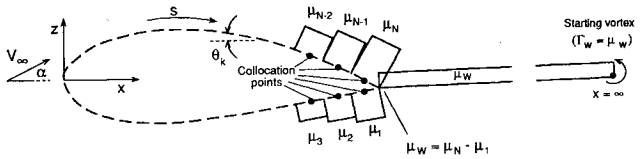

Fig. 2 Representation of the solution by a discrete set of surface source/doublet elements with constant strength.

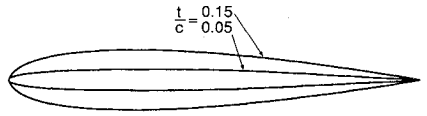

Fig. 3 Description of the geometry of 5% and a 15% thick van de Vooren airfoils.

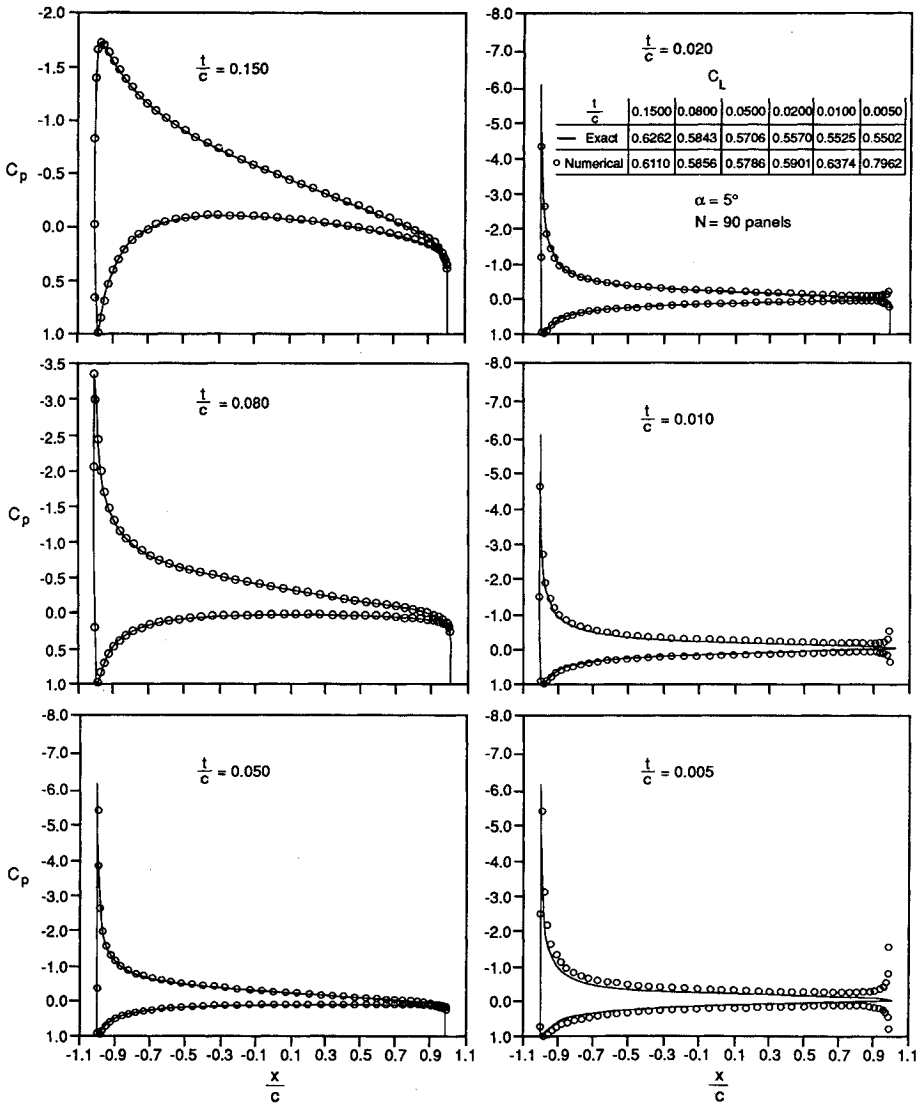

Fig. 4 Effect of airfoil thickness on the numerical solution of the pressure distribution on the van de Vooren airfoil (solution is based on constant-strength source/doublet elements using the internal Dirichlet boundary condition).

solid line stands for the exact solution, and the circles represent the numerical results. The upper case in Fig. 4 shows the 15% thick airfoil modeled by 90 panels, and the pressure distribution results agree well with the exact solution. This trend continues to 2% thick airfoils but breaks down near the trailing edge for thinner airfoils, such as the 0.5% thick airfoil shown in the figure (the percent means that maximum thickness over chord is $t/c = 0.005$). A comparison between the exact and computed lift coefficients is presented in the inset to Fig. 4 and the computed results were obtained by integrating the individual panel contributions. This table indicates, too, that for airfoils thicker than 2%, the integrated lift values differ only within a few percent from the exact values, whereas for thinner airfoils this difference increases considerably.

Figure 4 clearly demonstrates that for this airfoil when the thickness ratio is less than 2% the solution based on the Dirichlet boundary condition becomes inaccurate near the trailing edge. To investigate this problem further the pressure difference between the two trailing-edge panels vs trailing-edge thickness parameter is plotted in Fig. 5. The thickness parameter h/a is described in the inset to Fig. 5 and a is the distance between the two neighboring collocation points. Since the parameter h/a is directly related to the trailing-edge angle, this figure can be interpreted such that as trailing-edge angle approaches zero, the solution becomes unstable. Also, Eq. (11) indicates that the panel influence depends on the view angles θ and therefore the boundary condition at the two trailing-edge collocation points may yield an ill-conditioned problem. The effect of increasing the number of panels (or using smaller panels near the trailing edge) simply aggravates the problem and therefore larger trailing-edge panels usually can partially improve the solution.

In order to shed some light on the importance of the trailing-edge region to the numerical results, a comparison is made with the results for a similar airfoil but with a cusped trailing edge. The shape of this airfoil is similar to the previous airfoil (apart from the trailing-edge region), but its cusped trailing edge causes similar problems, even for the much thicker airfoil (see Fig. 6). The numerical problems associated with the solution of such airfoil shapes stimulated numerous studies, and two of the most recent ones are presented in Refs. 8 and 9.

Based on the information presented in Figs. 4 and 6, therefore, we can conclude that for lifting flows the trailing-edge thickness (or angle) is an important parameter and if $h/a < 0.25$ some numerical difficulties can be expected.

The effect of thickness on calculated lift and drag (where the latter should be zero) is plotted in Fig. 7. Here the aerodynamic coefficients are obtained by integration of the pressure distribution (to simulate commercial panel codes) and the magnitude of the error clearly increases for the thinner airfoils (similar results were reported in Ref. 10 which highlighted the possible large errors in the drag term). Again the effect of increased panel density increases the error and when using only 40 panels, from the engineering point of view, the results can be considered as reasonable.

It is clear that for zero-thickness lifting surfaces, different solution methods, based on the Neumann boundary condition, must be used so that this problem can be avoided (and in this case only one solid surface is specified, contrary to the thick airfoil case, where an upper and a lower surface are used). Also the various panel method formulations presented in Ref. 1 (Chap. 11) indicate that, in general, solutions based

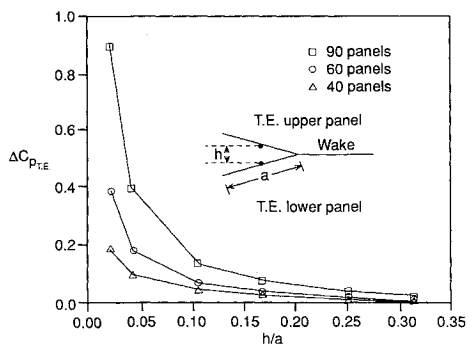

Fig. 5 Pressure difference between the trailing-edge upper and lower panels vs trailing-edge thickness parameter (or angle).

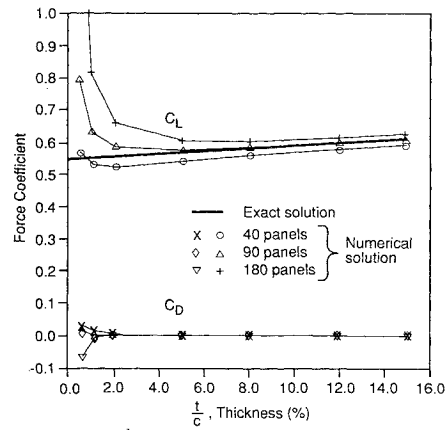

Fig. 7 Effect of thickness on computed lift and drag forces vs airfoil thickness ratio [for this solution the Kutta condition was specified by Eq. (7a)].

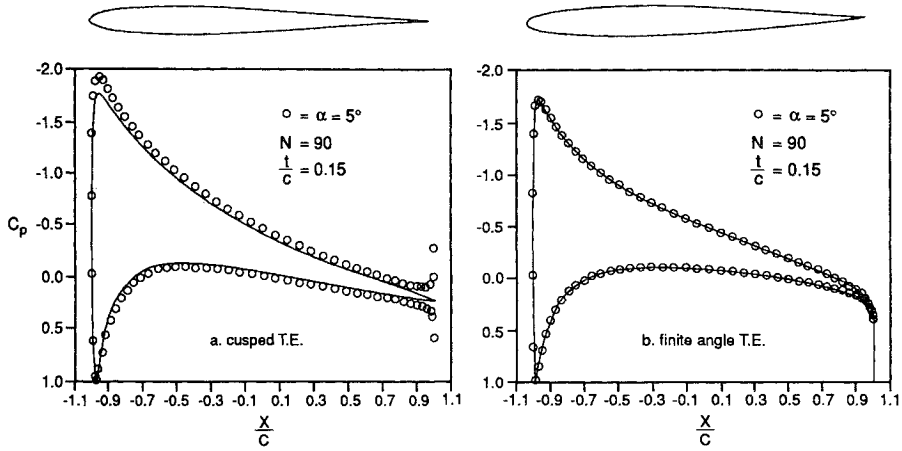

Fig. 6 Effect of a cusped trailing edge on the pressure distribution near the trailing edge. Both airfoils are van de Vooren airfoils (shown in the insets), but in case a, trailing edge angle is zero (cusped), and in case b, this angle is finite (actually $h/a = 0.31$, or $\theta = 17$ deg).

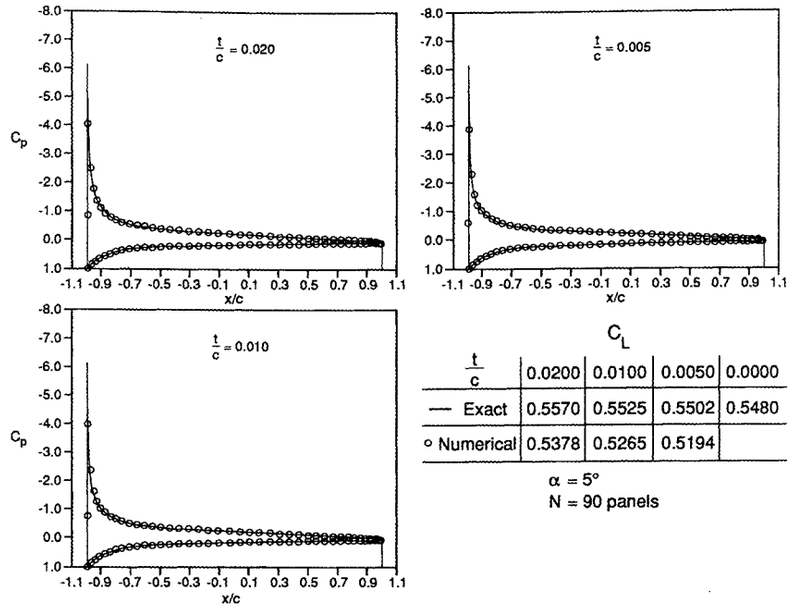

Fig. 8 The improved pressure distribution near the trailing edge for the last three cases presented in Fig. 4. For this solution the second form of the Kutta condition was used [Eq. (7b)].

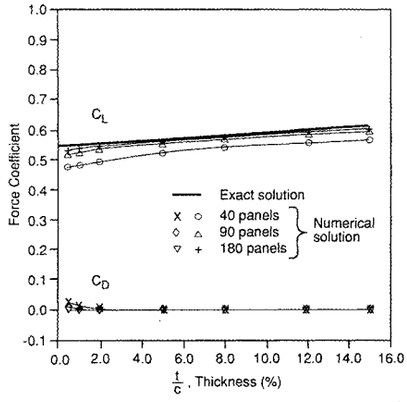

Fig. 9 Effect of thickness on computed lift-and drag forces vs airfoil-thickness ratio [the solution for this figure is based on the second form of the Kutta condition, Eq. (7b)].

on the Neumann boundary condition are less sensitive to this approaching-zero-thickness problem (excluding the constant doublet method). On the other hand, all Dirichlet boundary-condition-based methods were found to be susceptible to this trailing-edge instability. However, the problem being studied here relates to computer codes[4-6] used by the industry (which mostly use constant strength doublet/source elements and the Dirichlet boundary condition) and where the user finds it difficult to change the type of boundary conditions which were built into the program. Consequently, in this study only the effect of (two) minor programming changes were investigated which can be implemented easily with most panel codes. The first change requires a minor alteration in a wing trailing-edge geometry[8,9] such that the angle of the last two panels increases (thus the airfoil or wing is slightly different from the original one), and in this case satisfactory results were obtained (as long as $h/a > 0.25$ for the modified trailing edge panels, as indicated by the trends presented in Fig. 5).

The second modification requires the use of the velocity formulation for the Kutta condition [Eq. (7b)]. Such formulations were studied in the development stages of various panel methods,[11,12] but their numerical implementation caused, in some cases, an increase in the computational effort (results based on this approach are presented in Ref. 11 too, and they led to an improved pressure distribution near the trailing edge). In the present case the use of Eq. (7b) provided the $N + 1$th equation which for trailing-edge panels of equal length can be reduced to

$$\mu_N - \mu_{N-1} = \mu_1 - \mu_2 \tag{17}$$

This formulation of the last equation indeed extended the thickness range of the numerical solution. A repeat of the data of Fig. 4 is shown in Fig. 8 and for airfoils as thin as 0.5%, reasonable pressure distributions were obtained.

The results for lift and drag, when using the second form of the trailing-edge condition, are shown in Fig. 9, and the difference between the exact and calculated solutions is far less than in Fig. 7. More important is the fact that with more panels the solution improves and converges to the exact one. In conclusion, the use of Eq. (17) considerably improved the solution for lifting airfoils (and wings) with very thin trailing edges. However, the use of this type of Kutta condition instead of Eq. (7a) may increase computational effort for most panel codes [since the unknown wake doublet values μ_W cannot be resubstituted in a manner suggested by Eq. (7a)]. For example, when having N panels and N_W wake panel rows in a three-dimensional formulation, the use of Eq. (7a) results in a matrix equation of the order N, whereas the use of Eq. (7b) may yield a matrix of the order of $N + N_W$.

Concluding Remarks

Users of panel codes based on the Dirichlet boundary condition must be aware that when the trailing-edge thickness parameter becomes small ($h/a < 0.25$), then the numerical solution may become inaccurate.

The solution for thin wings (but not of zero thickness) when using a Dirichlet boundary-condition-based panel method can be improved by larger panels and by larger angles between these trailing-edge panels. Better results can be obtained by using an alternate form of the Kutta condition which requires that the upper and lower trailing-edge velocities be equal.

Acknowledgment

This work was supported by NASA Ames Research Center, under Grant NCC-2-596, with Dr. James C. Ross as project monitor.

References

[1]Katz, J., and Plotkin, A., *Low-Speed Aerodynamics: From Wing Theory to Panel Methods*, McGraw-Hill, New York, 1991.

[2]Morino, L., and Kuo, C. C., "Subsonic Potential Aerodynamics for Complex Configurations: A General Theory," *AIAA Journal*, Vol. 12, No. 2, 1974, pp. 191–197.

[3]Maskew, B., "Prediction of Subsonic Aerodynamic Characteristics: A Case for Low-Order Panel Methods," *AIAA Journal*, Vol. 19, No. 2, 1982, pp. 157–163.

[4]Youngren, H. H., Bouchard, E. E., Coopersmith, R. M., and Miranda, L. R., "Comparison of Panel Method Formulations and its Influence on the Development of QUADPAN, an Advanced Low-Order Method," AIAA Paper 83-1827, 1983.

[5]Maskew, B., "Program VSAERO Theory Document," NASA CR 4023, Sept. 1987.

[6]Ashby, L. D., Dudley, M. D., Iguchi, S. K., Browne, L., and Katz, J., "Potential Flow Theory and Operation Guide for the Panel Code PMARC," NASA TM 102851, March 1990.

[7]Kellogg, O. D., *Foundations of Potential Theory*, Dover Publishing Co., New York, 1953.

[8]Ardonceau, P. L., "Computation of the Potential Flow over Airfoils with Cusped or Thin Trailing Edges," *AIAA Journal*, Vol. 24, No. 8, 1986, pp. 1375–1377.

[9]Dutt, H. N. V., "Comment on 'Computation of the Potential Flow over Airfoils with Cusped or Thin Trailing Edges,' " *AIAA Journal*, Vol. 26, No. 1, 1988, pp. 122–123.

[10]Letcher, J. S. Jr., "Convergence of Lift and Drag Predictions by a Morino Panel Method (VSAERO)," *AIAA Journal*, Vol. 27, No. 8, 1989, pp. 1019–1020.

[11]Hess, J. L., "Panel Methods in Computational Fluid Dynamics," *Annual Review of Fluid Mechanics*, Vol. 22, 1990, pp. 262–263.

[12]Thomas, J. L., Luckring, J. M., and Sellers, W. L., "Evaluation of Factors Determining the Accuracy of Linearized Subsonic Panel Methods," AIAA Paper 83-1826, July 1983.